Spatial Scales of Stress-Carrying Nearshore Turbulence*

JOHN TROWBRIDGE AND STEVE ELGAR

Woods Hole Oceanographic Institution, Woods Hole, Massachusetts

(Manuscript received 5 November 2001, in final form 27 November 2002)

ABSTRACT

Measurements from a horizontal array of velocity sensors indicate that the alongshore scales of turbulence contributing to the near-bottom Reynolds stress just seaward of the surf zone on an ocean beach range from 0 to approximately 4 times the height of the measurements above the seafloor, with shorter scales during stable stratification than during neutral or unstable stratification. The dependence of alongshore turbulence scales on the stratification, Reynolds stress, and height above the bottom is consistent with semiempirical results from the atmospheric surface layer, implying similar dynamics of near-boundary turbulence in the atmosphere and the shallow coastal ocean.

1. Introduction

Spatial scales of turbulence in the atmospheric boundary layer have been characterized for a range of conditions (Kaimal et al. 1972), but observations of turbulence scales in oceanic boundary layers have been limited to unstratified tidal flows (Soulsby 1977; Gross and Nowell 1983). Spatial scales of weak turbulence in a strong mean flow can be estimated from time series measurements at a single point by means of the frozen-turbulence hypothesis (Taylor 1938). In many oceanic environments, surface waves complicate the interpretation of point measurements (Lumley and Terray 1983), and determination of turbulence scales requires a spatial array of sensors.

In this study, observations from an array of velocity sensors are used to estimate scales of turbulence just seaward of the surf zone on an ocean beach. The array was designed to estimate a spatial structure function $D_{vw}(\Delta y)$, defined by

$$D_{vw}(\Delta y) = \overline{[v(\mathbf{x} + \mathbf{j}\Delta y, t) - v(\mathbf{x}, t)][w(\mathbf{x} + \mathbf{j}\Delta y, t) - w(\mathbf{x}, t)]}. \quad (1)$$

Here, $\mathbf{x}$ and (x, y, z) denote the position vector, with x positive onshore, y alongshore, and z positive upward and equal to zero at the bottom; Δy is the alongshore separation; $\mathbf{j}$ is a unit vector in the y direction; t is time; (U, V, W) is the velocity vector; (u, v, w) is the departure of the velocity vector from its hour-averaged value; and an overbar denotes an hour average.

The analysis is based on the assumption that velocity fluctuations with timescales of less than 1 h are caused by superposed surface waves and turbulence. At the scales resolved by the array, the operation of subtraction in (1) largely removes effects of waves (Trowbridge 1998). In principle, $D_{vw}(\Delta y)$ increases from zero to $2\overline{v'w'}$, where primes denote turbulent fluctuations, as Δy increases from zero to values greater than the correlation scale of the turbulence. Thus, $D_{vw}(\Delta y)$ describes the alongshore scales of the turbulence contributing to the Reynolds shear stress $-\rho_0\overline{v'w'}$, where ρ is the density and the subscript 0 denotes a fixed reference value. This component of the Reynolds stress is a dominant term in the alongshore momentum balance in shallow water (Longuet-Higgins 1970; Feddersen et al. 1998; Lentz et al. 1999).

The null hypothesis is that the dynamics of turbulence in the shallow coastal ocean, at heights above bottom that are small relative to the water depth, but larger than the thickness of the oscillatory boundary layer produced by surface waves, are consistent with local application of Monin–Obukhov scaling (Monin and Yaglom 1971). In this scaling, the statistical properties of the velocity and density depend only on z, ρ_0, the vertical buoyancy

* Woods Hole Oceanographic Institution Contribution Number 10558.

Corresponding author address: John Trowbridge, Woods Hole Oceanographic Institution, Woods Hole, MA 02543.
E-mail: trowbridge@whoi.edu

flux $B = (g/\rho_0)\overline{\rho' w'}$, where g is gravity, and the vertical flux of streamwise momentum, here approximated by $\rho_0 \overline{v' w'}$, because hour-averaged currents at the measurement position were predominantly shore parallel, so that $\overline{U} \ll \overline{V}$ and $\overline{u' w'} \ll \overline{v' w'}$. Dimensional consistency requires that properly scaled statistics of the velocity and density fields be functions of z/L, where $L = |\overline{v' w'}|^{3/2}/(\kappa B)$ is the Monin–Obukhov length, with the empirical von Kármán constant $\kappa \simeq 0.40$. Monin–Obukhov scaling implies that

$$\frac{L_c}{z} = \phi\left(\frac{\kappa^2 z^2 N^2}{|\overline{v' w'}|}\right), \tag{2}$$

where L_c is a length characterizing the alongshore correlation scale of the stress-carrying turbulence, ϕ is a function that can be derived from semiempirical results obtained in the atmospheric surface layer, and $N^2 = -(g/\rho_0)\partial\overline{\rho}/\partial z$ is the squared buoyancy frequency, which can be positive or negative. Here, oceanic measurements of D_{vw} and z are fit to a model to determine $\overline{v' w'}$ and L_c, and these estimates are combined with measurements of N^2 to test (2).

2. Methods

a. Measurements

Four acoustic Doppler velocimeters (ADVs) were deployed in an alongshore array on a nearly planar sand beach, with a slope of approximately 0.03, about 60 m north of the pier at the Scripps Institution of Oceanography in La Jolla, California (Fig. 1). The ADVs were mounted on a low-profile, bottom-mounted frame, in an upward-looking orientation, with sample volumes about 0.75 m above the bottom. The ADV array permits estimates of D_{vw} at six nonzero equally spaced separations ranging from $\Delta y = 0.5$ m to $\Delta y = 3.0$ m. A pressure sensor was buried 0.3 m beneath the seafloor approximately 3 m from the center of the ADV array. A pair of sonar altimeters and a pair of temperature sensors were deployed approximately 10 m from the center of the ADV array (Fig. 1). The temperature sensors were 0.10 m above the ADV sample volumes. Ten-minute time-lapse video images obtained hourly (Holman et al. 1993) allowed the extent of the surf zone to be determined during daylight hours.

Sequential 1-h time series sampled at 8 Hz were obtained from each sensor between 19 October 2000 (yearday 295) and 7 January 2001 (yearday 369), shortly before the ADVs were buried by sand on 14 January 2001. Observations by divers indicate that the ADVs were occasionally fouled by kelp, and comparison of the hour-averaged temperature records indicates that the temperature sensors occasionally drifted. Hour-long records from a particular ADV were identified as having been fouled by kelp if the mean or standard deviation of any velocity component from that sensor differed by more than 0.01 m s^{-1} from the corresponding array

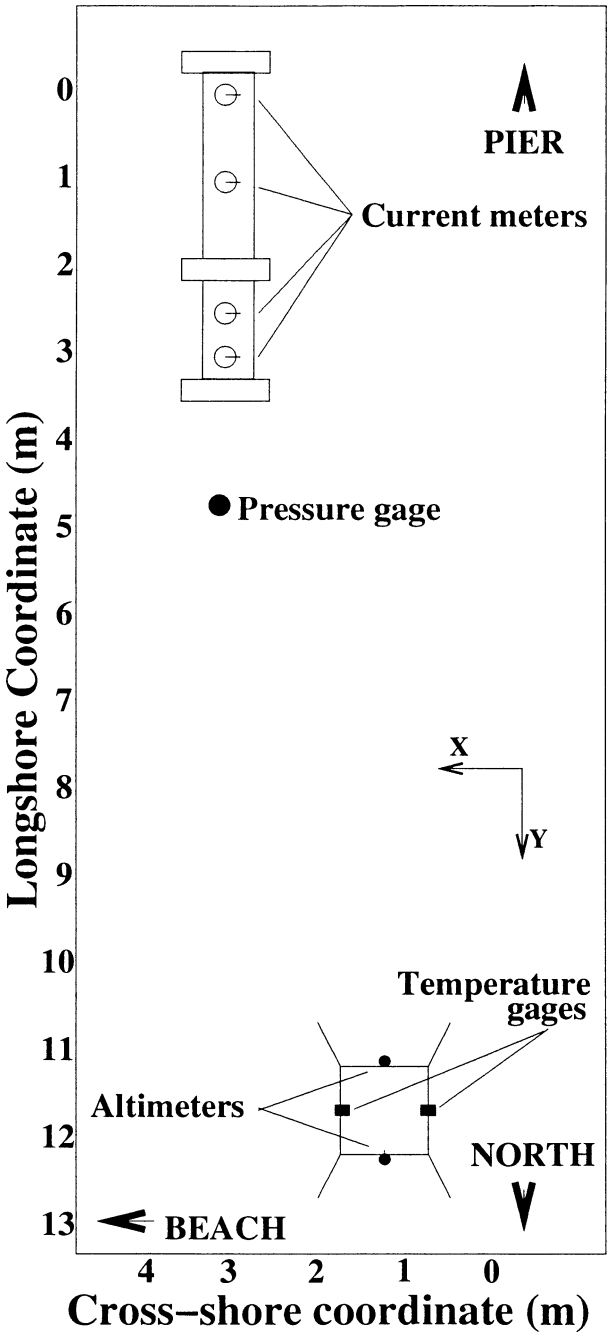

FIG. 1. Plan view of sensor array. The four ADVs (SonTek/YSI, Inc., ''OCEAN'' probes) were deployed in an alongshore array in approximately 4-m water depth, about 60 m north of the Scripps pier at La Jolla, CA. The acoustic altimeters provide estimates of the seafloor elevation, and the pressure gauge (buried in the sand to reduce flow noise) measures bottom pressure, which can be converted to sea surface elevation using linear wave theory. The temperature measurements were used to estimate the squared buoyancy frequency, as described in the text.

average. The results presented here are based on 854 1-h records for which all four ADVs were above sand level, none of the ADVs was fouled by kelp, and the two hour-averaged temperature measurements were within 0.1°C of each other. Video images indicate that the array was seaward of the surf zone during these records.

b. Models of D_{vw}, L_c/z, and N^2

A representation of D_{vw} follows from a semiempirical expression for the cospectrum of streamwise and vertical velocities in the atmospheric surface layer, given by

$$\frac{k_y \mathrm{Co}_{vw}(k_y)}{\overline{v'w'}} = \frac{7}{6\pi}\sin\left(\frac{3\pi}{7}\right)\frac{k_y L_c}{1 + |k_y L_c|^{7/3}}. \quad (3)$$

The coordinate system is defined so that the y axis is aligned with the mean velocity; Co_{vw} is the cospectrum of v and w, defined so that $\int_{-\infty}^{+\infty} \mathrm{Co}_{vw}(k_y)\, dk_y = \overline{v'w'}$; k_y is the y component of the radian wavenumber; and L_c is given by

$$\frac{L_c}{z} = \begin{cases} 1.2 & \text{for } z/L \le 0 \\ 1.2(1 + 7.9z/L)^{-3/4} & \text{for } 0 \le z/L. \end{cases} \quad (4)$$

The Fourier transform of $\mathrm{Co}_{vw}(k_y)$ is $E_{vw}(\Delta y)$, defined to be the even part of $\overline{v(\mathbf{x}, t)w(\mathbf{x} + \mathbf{j}\Delta y, t)}$ (Monin and Yaglom 1975). By definition, $D_{vw}(\Delta y) = 2[E_{vw}(0) - E_{vw}(\Delta y)]$. It follows that (3) is equivalent to

$$D_{vw}(\Delta y) = 2\overline{v'w'}\left[1 - \frac{7}{6\pi}\sin\left(\frac{3\pi}{7}\right)\int_{-\infty}^{+\infty}\cos\left(\xi\frac{\Delta y}{z}\frac{z}{L_c}\right)\frac{d\xi}{1 + |\xi|^{7/3}}\right], \quad (5)$$

where ξ is a dummy variable of integration. Equations (3) and (4) are similar to a model proposed by Kaimal et al. (1972) for neutral and stable stratification ($B \ge 0$), and they are consistent with theory and measurements at large k_y for both $B < 0$ and $B \ge 0$ (Kaimal et al. 1972; Wyngaard and Cote 1972). The integral on the right side of (5) depends only on the ratio of $\Delta y/z$ to L_c/z and can be evaluated numerically. According to (5), D_{vw} increases monotonically with Δy and is within 10% of $2\overline{v'w'}$ for $\Delta y \ge 3L_c$.

Standard results for the atmospheric surface layer lead to an expression for the squared buoyancy frequency (Hogstrom 1988):

$$\frac{\kappa^2 N^2 z^2}{|\overline{v'w'}|} = \begin{cases} 0.95z/L(1 - 11.6z/L)^{-1/2} & \text{for } z/L \le 0 \\ z/L(0.95 + 7.8z/L) & \text{for } 0 \le z/L. \end{cases} \quad (6)$$

Equations (4) and (6) define ϕ in (2).

c. Analysis

Structure functions were computed for each record at each of the six nonzero spatial separations by removing the hour average of alongshore and vertical velocity, computing products according to (1), and averaging over the 1-h record. Estimates of z and the mean water depth h were obtained from the altimeter and pressure measurements. Estimates of wave statistics were obtained from the pressure and velocity measurements using linear wave theory.

Estimates of $\partial\overline{T}/\partial z$, where T is the temperature, were obtained by regressing array-averaged estimates of $\partial T/\partial t$, obtained from centered differences of the temperature time series, against array-averaged measurements of $-w$. This procedure is based on a linearized model of temperature fluctuations given by

$$\frac{\partial T}{\partial t} + w\frac{\partial \overline{T}}{\partial z} = 0. \quad (7)$$

Both the variance of w and the covariance of $\partial T/\partial t$ and w were dominated by surface wave fluctuations at frequencies between approximately 0.05 and 0.5 Hz. The standard deviation of w was much larger than the bottom slope times the standard deviation of u, which suggests that estimates of $\partial\overline{T}/\partial z$ were not affected significantly by terms neglected in (7), such as $u\partial T/\partial x$, or by uncertainties in the orientation of the ADVs. The squared buoyancy frequency was estimated from $\partial\overline{T}/\partial z$ by assuming a linear relationship between temperature and density, with a slope of 0.24 kg $(\mathrm{m}^3\ ^\circ\mathrm{C})^{-1}$, determined from previous temperature and salinity observations near the measurement site (Lerczak 2000).

Estimates of $\overline{v'w'}$ and L_c/z were obtained by fitting measurements of D_{vw} to (5), with the measured $z/\Delta y$, using iterative least squares regression. First, the 854×6 measurements of D_{vw} were regressed against (5) to produce 854 preliminary estimates of $\overline{v'w'}$ and a single estimate of L_c/z, representative of the entire measurement period. The measured z and N^2 and the preliminary estimates of $\overline{v'w'}$ were then used to compute $\kappa^2N^2z^2/|\overline{v'w'}|$ for each 1-h record. To exclude observations in which $\overline{v'w'}$ was too small to be estimated accurately, 54 1-h records for which $|\kappa^2N^2z^2/\overline{v'w'}| > 2$ were omitted from the analysis. The remaining 800 records were sorted into four equally sized groups in order of increasing $\kappa^2N^2z^2/|\overline{v'w'}|$. The 200×6 measurements of D_{vw} within each group were then regressed against (5) to produce 200 final estimates of $\overline{v'w'}$ and a single estimate of L_c/z for that

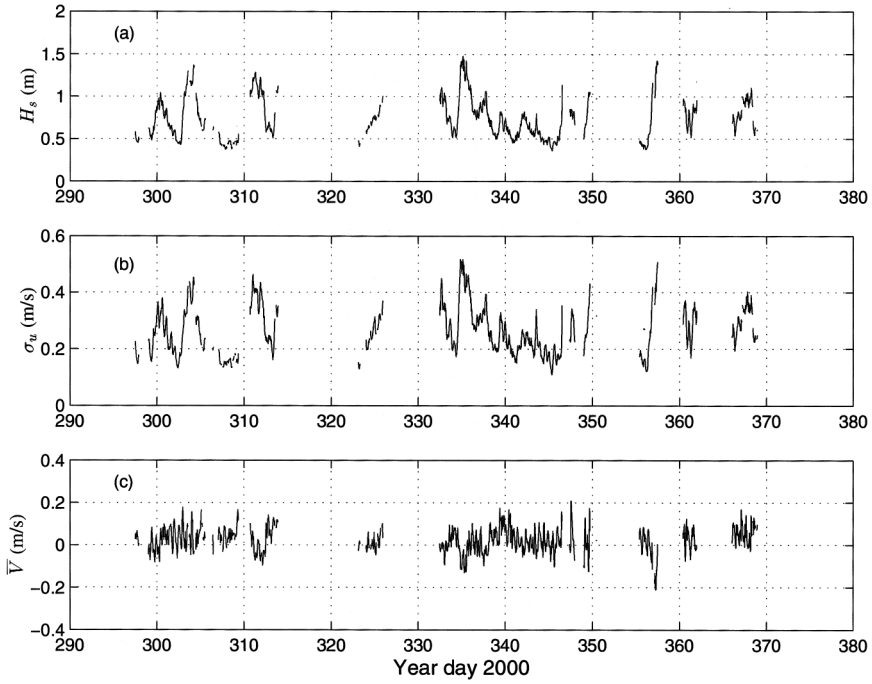

FIG. 2. Time series of (a) significant wave height H_s, (b) std dev σ_u of the cross-shore velocity, and (c) alongshore velocity $\overline{V}$. All statistics are hour averages. Only the records with valid data, as defined in the text, are included. Significant wave height is defined to be 4 times the standard deviation of the surface displacement and was estimated from pressure measurements by means of linear wave theory. Gaps in the time series are caused by fouling owing to kelp, a power failure, and drift in the temperature sensors. All records used in the analysis have identical gaps.

group. The preliminary and final estimates of $\overline{v'w'}$ were not significantly different. The result of this procedure was four estimates of L_c/z, ordered by $\kappa^2N^2z^2/|\overline{v'w'}|$, and 800 estimates of $\overline{v'w'}$. Error bounds for L_c/z were obtained by a standard procedure based on Gaussian statistics and linearization of the nonlinear regression about the best-fit values of the parameters (e.g., Draper and Smith 1966). In the calculation of error bounds, the six measurements of D_{vw} obtained during each 1-h record were assumed to have only 2 degrees of freedom, because concurrent measurements of D_{vw} at different spatial separations were not statistically independent (e.g., Cressie 1993).

3. Results

During the 70-day measurement period, the significant wave height ranged from approximately 0.5 to 1.5 m, the standard deviation of the cross-shore velocity ranged from approximately 0.2 to 0.5 m s^{-1}, and the hour-averaged alongshore velocity usually was less than 0.1 m s^{-1}, with maximum values of about 0.2 m s^{-1} (Fig. 2). Hour-averaged cross-shore velocities were much smaller than hour-averaged alongshore velocities. Wave incidence angles were within 10° of shore normal. The mean and standard deviation of $\partial\overline{T}/\partial z$ were -0.01° and 0.03°C, respectively. Stable stratification usually occurred during southward alongshore flows ($\overline{V} < 0$), and unstable stratification usually occurred during northward alongshore flows ($\overline{V} > 0$). The hour-averaged water depth varied between approximately 3.0 and 5.5 m, primarily owing to tidal fluctuations. The height of the velocity measurements above the bottom ranged between 0.75 and 0.93 m as the seafloor eroded and accreted. The measurement height z was larger than the thickness of the oscillatory boundary layer produced by surface waves, estimated at a few centimeters (Grant and Madsen 1979) but was small in comparison with the hour-averaged water depth h ($0.15 < z/h < 0.30$). Approximately 60% of the variance of the alongshore current was at frequencies below 2 cycles per day, approximately 20% was at semidiurnal frequencies, and the remaining 20% was at frequencies greater than semidiurnal.

Visual observations obtained nearly daily by divers suggest that the seafloor was smooth, with no signs of wave-orbital or larger-scale ripples or bedforms. The seafloor elevation varied by centimeters on timescales of hours, but the differences between the two altimeters indicate there were no bedforms with horizontal scales smaller than the altimeter spacing and vertical scales larger than the altimeter accuracy of about 0.01 m (Gallagher et al. 1998).

The qualitative dependence of the measured structure functions on spatial separation and stratification is consistent with expectations (Fig. 3). The magnitude of D_{vw}

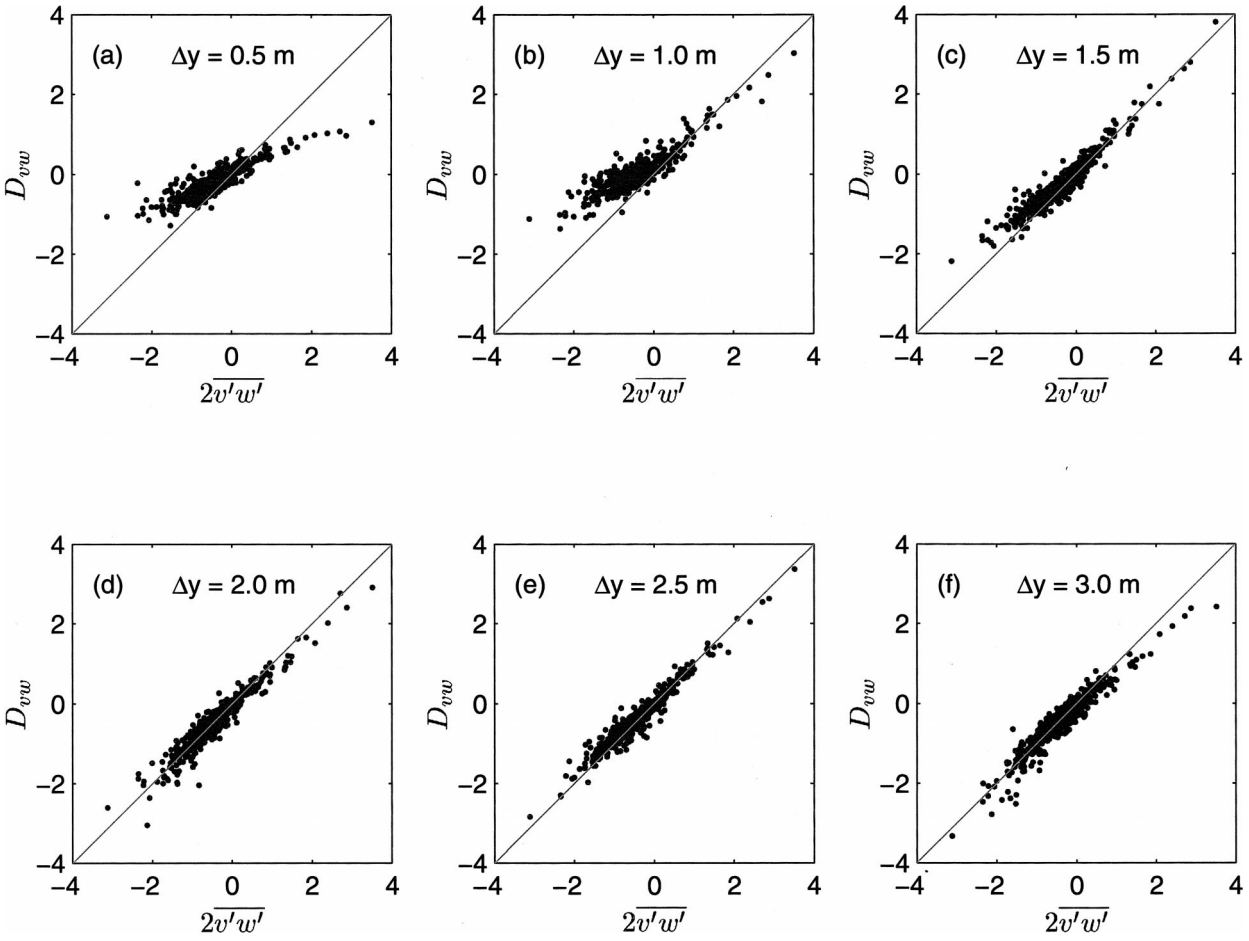

FIG. 3. Structure function D_{vw} for different spatial separations vs $2\overline{v'w'}$. Units: 10^{-4} m^2 s^{-2}.

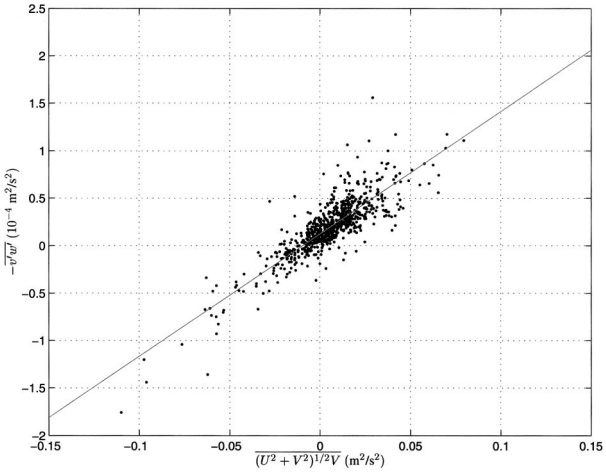

FIG. 4. Estimates of $-\overline{v'w'}$ vs $\overline{(U^2 + V^2)^{1/2}V}$. The estimate of the drag coefficient, defined to be the slope of the best-fit straight line through the relationship between $-\overline{v'w'}$ and $\overline{(U^2 + V^2)^{1/2}V}$, is $(1.3 \pm 0.1) \times 10^{-3}$ at 95% confidence. It is not known why the observed relationship between $-\overline{v'w'}$ and $\overline{(U^2 + V^2)^{1/2}V}$ has a nonzero intercept.

is smaller than $2\overline{v'w'}$ at small Δy, and it asymptotically approaches $2\overline{v'w'}$ as Δy increases. The approach of D_{vw} to $2\overline{v'w'}$ with increasing Δy is more rapid for positive $\overline{v'w'}$, corresponding to $\overline{V} < 0$ and stable stratification, than it is for negative $\overline{v'w'}$, corresponding to $\overline{V} > 0$ and unstable stratification. The alongshore turbulence scales suggested by Fig. 3 are roughly 1.0 m for stable stratification and are between about 1.5 and 2.5 m for unstable stratification.

Estimates of $\overline{v'w'}$ are approximately consistent with a quadratic drag law, given by

$$-\overline{v'w'} = c_d\overline{(U^2 + V^2)^{1/2}V}, \tag{8}$$

with a drag coefficient $c_d = (1.3 \pm 0.1) \times 10^{-3}$ at 95% confidence (Fig. 4), which is similar to previous estimates of the drag coefficient in nearshore flows under unbroken waves (Feddersen et al. 1998; Trowbridge and Elgar 2001).

The dependence of L_c/z on $\kappa^2N^2z^2/|\overline{v'w'}|$ indicates suppression of turbulence scale by stable stratification and agreement with the atmospheric results in (4) and (6) (Fig. 5). Corresponding estimates of the drag co-

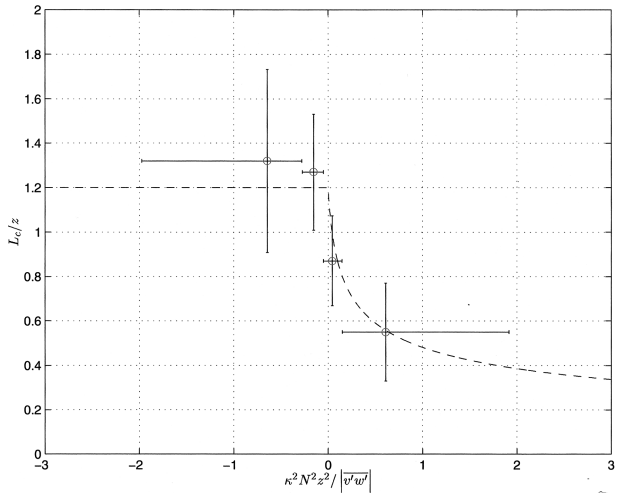

FIG. 5. Dimensionless length-scale parameter L_c/z vs dimensionless stratification parameter $\kappa^2 N^2 z^2/|\overline{v'w'}|$. The circles are estimated from the measurements, and the dashed curve is the atmospheric result given by (4) and (6). The horizontal error bars represent the range of stratification parameter that was used to obtain the averaged estimates of L_c/z. The vertical error bars represent approximate 95% confidence limits, estimated as explained in the text. The measurements indicate a reduction in length scale with increasing stratification parameter, in agreement with the atmospheric results. The stratification parameter changes sign because N^2 can be positive or negative.

efficient indicate no significant dependence on $\kappa^2 N^2 z^2/|\overline{v'w'}|$.

4. Discussion

The observations indicate that turbulence length scales in the shallow coastal ocean, at heights above the bottom that are small in comparison with the water depth but are larger than the thickness of the wave boundary layer, are influenced by stratification in a manner consistent with local application of Monin–Obukhov scaling (Fig. 5). This result implies that the dynamics of near-boundary turbulence in the shallow coastal ocean and the atmosphere are similar, even though the environments differ. In the atmospheric surface layer, both $\overline{v'w'}$ and B are nearly independent of z. At water depths of a few meters seaward of the surf zone in the ocean, scaling and measurements (Feddersen et al. 1998; Lentz et al. 1999) indicate that Coriolis acceleration is negligible in the hour-averaged alongshore momentum balance and that the dominant terms in the depth-integrated balance are wind stress and bottom stress, implying that $\overline{v'w'}$ is nearly independent of z, as in the atmospheric surface layer. However, the seafloor usually is idealized as nonconducting for both heat and salt, so that $B \to 0$ as $z \to 0$, and thus B must vary with z if $B \neq 0$. The present results indicate that the dependence of B on z does not have a dominant effect on the local dynamics of the turbulence.

For a fixed turbulent Reynolds shear stress, increasing stable stratification reduces the eddy viscosity and increases the vertical derivative of the hour-averaged velocity. Measurements in the atmospheric surface layer indicate that (Monin and Yaglom 1971)

$$\frac{\partial \overline{V}}{\partial z} = \frac{1}{\kappa z}|\overline{v'w'}|^{1/2}\,\mathrm{sign}(\overline{v'w'})\left(1 + \beta\frac{z}{L}\right), \qquad (9)$$

where β is an empirical constant, approximately equal to 6.0 (Hogstrom 1988). For the observations used here, z/L was as large as 0.3, which corresponds in (9) to a reduction in eddy viscosity and an increase in $\partial\overline{V}/\partial z$ by a factor of 2.5. Measurements of $\overline{V}(z)$ often are fit to (9) to infer $\overline{v'w'}$. In the present case, this procedure would result in overestimates of $\overline{v'w'}$ by factors of roughly 6 during stable stratification.

The measurements indicate a 50% reduction in length scale during stable stratification (Fig. 5) but no significant dependence of the drag coefficient on stratification (section 3). This result is consistent with local application of Monin–Obukhov scaling. A simple model for near-bottom flow in the ocean, where $B \to 0$ as $z \to 0$, is $\overline{v'w'}$ = constant and $B = z\partial B/\partial z$, where $\partial B/\partial z$ = constant. For this case, integration of (9) with respect to z gives

$$\overline{V} = \frac{1}{\kappa}|\overline{v'w'}|^{1/2}\,\mathrm{sign}(\overline{v'w'})\left[\log\left(\frac{z}{z_0}\right) + \frac{\beta}{2}\frac{z}{L}\right], \qquad (10)$$

where z_0 is the bottom roughness length, which includes the effect of the bottom boundary layer produced by surface waves (Grant and Madsen 1979). For the data discussed here, the second term in square brackets in (10) is substantially smaller than the first, so that stratification has a small effect on the local relationship between the hour-averaged velocity and the turbulent Reynolds shear stress, even though it has an important effect on the vertical gradient of the hour-averaged velocity in (9).

Divergence from Monin–Obukhov scaling at small k_y is observed in atmospheric measurements during unstable conditions ($B < 0$) and is attributed to large-scale, convective circulations driven by the unstable density structure (Kaimal et al. 1972), which presumably depend on scales in addition to B, $\overline{v'w'}$, and z. Here, the manifestation of similar processes would be L_c/z larger than predicted by (4) and (6) at large, negative $\kappa^2 N^2 z^2/|\overline{v'w'}|$. This behavior is suggested by the measurements (Fig. 5), but the uncertainty is sufficiently large that the observations are not necessarily inconsistent with (4) and (6).

The alongshore turbulence scale during unstable stratification was the same order of magnitude as the water depth h (Figs. 3 and 5), but h is unlikely to have placed an important constraint on turbulence scale at the measurement height. The quantity z/h, a dimensionless measure of the importance of h, was small, and the measurements indicate no systematic dependence of L_c/z on z/h. This result is consistent with laboratory measurements in open channels indicating that the water depth

affects the turbulence scales only for $z/h > 0.5$ (Nezu and Nakagawa 1993). Also, much of the energy appearing at long spatial scales in turbulence statistics referenced to a single coordinate direction, such as $D_{vw}(\Delta y)$ and $\mathrm{Co}_{vw}(k_y)$, is aliased from shorter scales, because wavelengths of individual Fourier components appear longer if the wavenumber is not aligned with the coordinate direction of interest. Thus, the actual scale of the stress-carrying turbulence was smaller than $3L_c$, the value of Δy for which D_{vw} is within 10% of $2\overline{v'w'}$.

The wave-induced strain rate (of order $k\sigma_u$, where k is the wavenumber of the surface waves and σ_u is the standard deviation of u), was larger than the strain rates of the hour-averaged velocity field and the stress-carrying turbulence (both of order $|\overline{v'w'}|^{1/2}/z$), but straining by the wave-induced velocity field is unlikely to have had an important effect on the turbulence at the measurement position. The measurements indicate no systematic dependence of L_c/z on $k\sigma_u z/|\overline{v'w'}|^{1/2}$, the ratio of wave-induced to turbulent strain rates. The wave-induced strain rate is oscillatory and therefore is unlikely to have had an important effect when averaged over many wave periods. Also, an order-of-magnitude argument adapted from Phillips (1961) indicates that wave-induced straining of turbulence had a negligible effect on the hour-averaged budget for the turbulent vorticity variance. Although it does not directly address stress-carrying scales, the argument of Phillips (1961) suggests that wave-induced straining had a minor effect on the turbulence.

5. Conclusions

Measurements from an alongshore array of near-bottom velocity sensors located approximately 0.8 m above the seafloor in 4-m water depth on an ocean beach were used to estimate the alongshore scales of the turbulent Reynolds stress just seaward of the surf zone. The analysis is based on a spatial structure function that rejects contributions from waves. Estimates of Reynolds stress are consistent with a quadratic drag law, with a drag coefficient similar to previous observational estimates. Turbulent length scales were approximately 2 m during unstable stratification and were reduced by a factor of roughly 2 during stable stratification, in a manner consistent with atmospheric results based on Monin–Obukhov scaling. Effects of finite water depth and straining of turbulence by the wave-induced velocity field were small. The results imply that turbulence in the shallow coastal ocean, just above the oscillatory bottom boundary layer produced by surface waves, is dynamically similar to turbulence in the atmospheric surface layer.

Acknowledgments. Support was provided by the Office of Naval Research (Marine Geology and Geophysics and Ocean Modeling and Prediction programs) and the National Science Foundation. Britt Raubenheimer helped to design, deploy, and maintain the sensor arrays, contributed significantly to the data analysis, and provided valuable comments. Staff from the Center for Coastal Studies at the Scripps Institution of Oceanography deployed the arrays and kept them operational despite nearly continuous attacks by kelp in cold water with large waves. Janet Fredericks did the preliminary data processing. Steve Lentz and two anonymous reviewers provided insightful comments on an early draft.

REFERENCES

Cressie, N. A. C., 1993: *Statistics for Spatial Data.* John Wiley and Sons, 900 pp.

Draper, N. R., and H. Smith, 1966: *Applied Regression Analysis.* John Wiley and Sons, 407 pp.

Feddersen, F., R. T. Guza, S. Elgar, and T. H. C. Herbers, 1998: Alongshore momentum balances in the nearshore. *J. Geophys. Res.,* **103,** 15 667–15 676.

Gallagher, E., S. Elgar, and E. B. Thornton, 1998: Megaripple migration in a natural surfzone. *Nature,* **394,** 165–168.

Grant, W. D., and O. W. Madsen, 1979: Combined wave and current interaction with a rough bottom. *J. Geophys. Res.,* **84,** 1979–1808.

Gross, T. F., and A. R. M. Nowell, 1983: Mean flow and turbulence scaling in a tidal boundary layer. *Cont. Shelf Res.,* **2,** 109–126.

Hogstrom, U., 1988: Non-dimensional wind and temperature profiles in the atmospheric surface layer: A re-evaluation. *Bound.-Layer Meteor.,* **42,** 55–78.

Holman, R. A., A. H. Sallenger Jr., T. C. Lippmann, and J. Haines, 1993: The application of video image processing to the study of nearshore processes. *Oceanography,* **6,** 78–85.

Kaimal, J. C., I. Izumi, and O. R. Cote, 1972: Spectral characteristics of surface layer turbulence. *Quart. J. Roy. Meteor. Soc.,* **98,** 563–589.

Lentz, S., R. T. Guza, S. Elgar, F. Feddersen, and T. H. C. Herbers, 1999: Momentum balances on the North Carolina inner shelf. *J. Geophys. Res.,* **104,** 18 205–18 226.

Lerczak, J. A., 2000: Internal waves on the southern California shelf. Ph.D. thesis, University of California, San Diego, 244 pp.

Longuet-Higgins, M. H., 1970: Longshore currents generated by obliquely incident sea waves. *J. Geophys. Res.,* **75,** 6778–6789.

Lumley, J. L., and E. A. Terray, 1983: Kinematics of turbulence convected by a random wave field. *J. Phys. Oceanogr.,* **13,** 2000–2007.

Monin, A. S., and A. M. Yaglom, 1971: *Statistical Fluid Mechanics: Mechanics of Turbulence.* Vol. 1, MIT Press, 769 pp.

——, and ——, 1975: *Statistical Fluid Mechanics: Mechanics of Turbulence.* Vol. 2, MIT Press, 874 pp.

Nezu, I., and H. Nakagawa, 1993: *Turbulence in Open-Channel Flows.* A. A. Balkema Publishers, 281 pp.

Phillips, O. M., 1961: A note on the turbulence generated by gravity waves. *J. Geophys. Res.,* **66,** 2889–2893.

Soulsby, R. L., 1977: Similarity scaling of turbulence spectra in marine and atmospheric boundary layers. *J. Phys. Oceanogr.,* **7,** 934–937.

Taylor, G. I., 1938: The spectrum of turbulence. *Proc. Roy. Soc. London,* **A164,** 476–490.

Trowbridge, J. H., 1998: On a technique for measurement of turbulent shear stress in the presence of surface waves. *J. Atmos. Oceanic Technol.,* **15,** 290–298.

——, and S. Elgar, 2001: Turbulence measurements in the surf zone. *J. Phys. Oceanogr.,* **31,** 2403–2417.

Wyngaard, J. C., and O. R. Cote, 1972: Cospectral similarity in the atmospheric surface layer. *Quart. J. Roy. Meteor. Soc.,* **98,** 590–603.